

Preparation of New $Ba_4M_3S_{10}$ Phases ($M = Zr, Hf$) and Single Crystal Structure Determination of $Ba_4Zr_3S_{10}$

BAI-HAO CHEN,* WINNIE WONG-NG,† AND BRYAN W. EICHHORN*

*Center for Superconductivity Research and Department of Chemistry and Biochemistry, University of Maryland, College Park, Maryland 20742; and †National Institute of Standards and Technology, Gaithersburg, Maryland 20899

Received May 18, 1992; in revised form August 3, 1992; accepted August 5, 1992

Two new Ruddlesden–Popper $Ba_{n+1}M_nS_{3n+1}$ compounds where $M = Zr, Hf$ and $n = 3$ have been prepared in good yield from BaS , M , and S in a $BaCl_2$ flux at $1050^\circ C$. The structures comprise triple layer perovskite slabs separated by double BaS layers. The single crystal structure of $Ba_4Zr_3S_{10}$ revealed $Zr-S$ distances of $2.493(3)$ Å (average) with one long $Zr-S$ contact of $2.562(5)$ Å for the distal bond of the ZrS_6 octahedron at the perovskite/double BaS interface. The $Ba-S$ contacts average $3.52(1)$ Å inside the perovskite blocks and range between $3.084(5)$ and $3.552(1)$ Å in the double BaS layers. Crystal data for $Ba_4Zr_3S_{10}$ ($25^\circ C$) are $a = 7.0314(5)$ Å, $b = 7.0552(7)$ Å, $c = 35.544(7)$ Å, $Z = 4$, $D_{calc} = 4.038$ g/cm³, orthorhombic, space group $Fmmm$, $R(F) = 0.038$, $R_w(F) = 0.058$. Single crystals of $Ba_4Hf_3S_{10}$ were indexed on an orthorhombic cell with $a = 6.989(3)$ Å, $b = 7.022(2)$ Å, and $c = 35.428(8)$ Å but the structure was not refined due to poor quality data. © 1993 Academic Press, Inc.

Introduction

There is renewed interest in the preparation of new early transition metal sulfides with layered structures (1–4). We and others have recently reported (5–7) five members in a new series of perovskite-related $Ba_{n+1}M_nS_{3n+1}$ compounds ($M = Zr, Hf$) that adopt Ruddlesden–Popper (R–P) type structures (8). The recent discovery of superconductivity at 60 K in the R–P copper oxides, $La_{2-x}Sr_xCaCu_2O_6$ (9), has rekindled interest in the preparation of new oxides with this general structure type (10). The discovery of R–P sulfides is of interest due not only to the structural similarities of these compounds to the copper oxide superconductors but also due to the covalent two

dimensional bonding in the sulfides that contrasts with the ionic nature of the early transition metal oxide phases. We report here the preparation of two new R–P sulfides, namely, the $Ba_4M_3S_{10}$ compounds, where $M = Zr$ and Hf . A summary of structural data and a comparison of the structural features for the $Ba_{n+1}M_nS_{3n+1}$ series are also presented.

Experimental

(1) Synthesis

BaS , Hf powder, and elemental sulfur in a 3 : 2 : 4 ratio were ground and loaded into a silica ampule along with 15% $BaCl_2$ by weight. The tube was sealed under vacuum and placed inside a larger silica tube which

was also sealed under vacuum. The material was heated to 1050°C at 0.3°C/min and fired at 1050°C for an additional 20 hr. The sample was then quickly cooled to room temperature (2 hr). The resulting material was washed with water to dissolve the BaCl₂ flux leaving well formed dark orange-brown crystals of Ba₄Hf₃S₁₀ (ca. 75% of product mass) along with a lighter orange powder (ca. 25% of product mass). The synthesis of Ba₄Zr₃S₁₀ was identical to that just described except that Zr metal was employed. The Zr compound was also obtained as a dark orange-brown crystalline solid that constituted ca. 75% of the reaction mixture.

(2) X-Ray Structure Determination

A dark orange-brown brick of Ba₄Zr₃S₁₀ with crystal dimensions 0.18 × 0.13 × 0.04 mm was mounted in a Lindemann-type glass fiber in a random orientation. Data collection was performed at 25°C with MoK α radiation ($\lambda = 0.71073 \text{ \AA}$) on an Enraf-Nonius CAD4 computer-controlled kappa axis diffractometer equipped with a graphite crystal incident beam monochromator. Data were collected by using an $\omega/2\theta$ scan mode with a variable scan rate (0.7–4°/min). Periodic monitoring of three check reflections throughout data collection showed the crystal to be stable.

Cell constants and an orientation matrix for data collection were obtained from least-squares refinement, using setting angles of 25 reflections in the range $10^\circ < \theta < 20^\circ$, measured by the computer-controlled diagonal slit method of centering. The crystallographic data are summarized in Table I. A total of 982 reflections were collected between 0° and 56° in 2θ of which 738 were unique with 458 having $I \geq 3\sigma(I)$. The latter were used in refinement of the structure. Lorentz and polarization corrections were applied to the data. An empirical absorption correction (Ψ scan method) and a secondary extinction correction were applied. Atomic scattering factors were taken from Ref. (11).

TABLE I
CRYSTALLOGRAPHIC DATA FOR Ba₄Zr₃S₁₀

Formula weight (amu)	1143.66
$a(\text{\AA})$	7.0314(5)
$b(\text{\AA})$	7.0552(7)
$c(\text{\AA})$	35.544(7)
$V(\text{\AA}^3)$	1,763.3
$T(^{\circ}\text{C})$	25
Z	4
$D_{\text{cal}}(\text{g/cm}^3)$	4.038
Space group	<i>Fm</i> <i>mm</i> (#69)
Total no. refln.	982
No. unique refln.	738
No. refln. ($I > 3\sigma(I)$)	458
No. of variables	34
$\lambda(\text{\AA})$	0.71073
$\mu(\text{mm}^{-1})$	115.9
$R(F)^a$	0.038
$R_w(F)^a$	0.058
G.O.F.	1.94
Shift/error	0.03

$$^a R(F) = \Sigma|F_o - F_c|/\Sigma F_o; R_w(F) = (\Sigma w|F_o - F_c|^2 / \Sigma w F_o^2)^{1/2}.$$

The data were indexed on a face centered orthorhombic cell, displaying no additional systematic absences, consistent with space groups *F*222, *Fm*m2, and *Fm*mm. Solution and refinement in the higher symmetry space group *Fm*mm (#69) confirmed the latter as the correct choice. The initial atomic coordinates were estimated using idealized positions based on a standard Ruddlesden-Popper type structure. The structure was successfully refined (MOLEN, Enraf-Nonius) in full-matrix least squares with all atoms anisotropic in the final cycles. The final residuals were $R(F) = 3.8\%$ and $R_w(F) = 5.8\%$. The non-Poisson weighting scheme with $\rho = 0.04$ was used. The highest peak in the final difference map was 0.6 e/\AA^3 .

Atom S(3), which resides on a Wyckoff 8e site, appears to have a large temperature factor (9.0 \AA^2) relative to the other atoms in the structure. The high value is not likely the result of an origin problem, which would also affect the other atoms, or a disorder

TABLE II
FRACTIONAL COORDINATES AND THERMAL PARAMETERS (\AA^2) FOR $Ba_4Zr_3S_{10}$

Atom	Wyckoff site	x	y	z	B_{11}	B_{22}	B_{33}	B_{12}	B_{13}	B_{23}	B_{eqv}
Zr(1)	4a	0	0	0	0.9(1)	1.21(6)	0.75(6)	0	0	0	0.95(4)
Zr(2)	8i	0	0	0.14225(4)	1.68(9)	1.65(5)	0.04(4)	0	0	0	1.42(3)
Ba(1)	8i	$\frac{1}{2}$	0	0.06983(3)	3.15(8)	2.51(4)	1.41(3)	0	0	0	2.36(3)
Ba(2)	8i	$\frac{1}{2}$	0	0.20080(3)	2.31(7)	2.48(4)	0.86(3)	0	0	0	1.89(2)
S(1)	8i	0	0	0.0702(1)	5.3(5)	9.9(5)	0.4(1)	0	0	0	5.2(2)
S(2)	8i	0	0	0.2124(1)	3.8(4)	6.5(3)	0.6(1)	0	0	0	3.7(2)
S(3)	8e	$\frac{1}{4}$	$\frac{1}{4}$	0	9.5(3)	9.9(3)	7.6(4)	-9.2(2)	0	0	9.0(2)
S(4)	16j	$\frac{1}{4}$	$\frac{1}{4}$	0.1392(1)	1.8(2)	1.58(9)	5.7(2)	-0.7(1)	0	0	3.04(8)

Note. The form of the anisotropic displacement parameter is $\exp[-0.25(h^2a^{*2}\beta_{11} + k^2b^{*2}\beta_{22} + l^2c^{*2}\beta_{33} + 2hka^*b^*\beta_{12} + 2hla^*c^*\beta_{13} + 2klb^*c^*\beta_{23})]$, where a^* , b^* , and c^* are reciprocal lattice constants.

problem. Attempts have been made to refine S(3) using partial occupancy which leads to higher R factors as well as nonpositive definite temperature factors. Moreover, the B_{11} , B_{22} , and B_{33} values are rather similar, indicating relatively isotropic motion. A few large temperature factors were also observed in the $Ba_6Hf_5S_{16}$ and $Ba_5Hf_4S_{13}$ refinements (7).

Results

Single crystals of $Ba_4Zr_3S_{10}$ and $Ba_4Hf_3S_{10}$ were obtained from sealed tube reactions incorporating 15 wt% $BaCl_2$ flux. Both reactions generated mixtures of products in which the title compounds constituted ca. 75% of the product mass. Powder X-ray diffraction (XRD) studies on the product mixtures revealed the presence of $Ba_{n+1}M_nS_{3n+1}$ type compounds ($n \geq 3$) and small amounts of BaS , but MS_2 or other impurities were not detected. The $Ba_{n+1}M_nS_{3n+1}$ compounds with $n \geq 3$ are difficult to differentiate from powder diffraction data (7).

Several crystals of both compounds were indexed by single crystal X-ray diffraction and all displayed characteristic $\sim 35 \text{ \AA}$ c axes indicative of $Ba_{n+1}M_nS_{3n+1}$ compounds with $n = 3$. Most of the crystals displayed broad diffraction peaks and did not yield satisfactory data sets for structure refinement. A

few of the Zr crystals diffracted well and a high quality data set was obtained and the structure refined. Several different $Ba_4Hf_3S_{10}$ crystals from different syntheses were indexed on an orthorhombic cell with $a = 6.989(3) \text{ \AA}$, $b = 7.022(2) \text{ \AA}$, and $c = 35.428(8) \text{ \AA}$ but the poor quality of the diffraction peaks precluded satisfactory structural refinement and accurate space group determination.

The $Ba_4Zr_3S_{10}$ compound is orthorhombic, with $a = 7.0314(5) \text{ \AA}$, $b = 7.0552(7) \text{ \AA}$, and $c = 35.544(7) \text{ \AA}$, and was successfully refined ($R(F) = 0.038$, $R_w(F) = 0.058$) in space group $Fmmm$. The fractional coordinates, anisotropic thermal parameters, and selected bond distances and angles are listed in Tables II and III. Attempted refinements in higher symmetry $I4/mmm$ symmetry were unsuccessful, as were attempted transformations of the refined structure into an $I4/mmm$ tetragonal cell [$R(F) > 0.29$].

The $Ba_4Zr_3S_{10}$ compound adopts a typical Ruddlesden-Popper structure and is shown in Fig. 1. The structure consists of $BaZrS_3$ perovskite slabs with corner-sharing $ZrS_{6/2}$ octahedra extending infinitely in the a - b plane and for three layers along c . The triple-layer perovskite slabs are separated by double BaS rock salt layers with each successive perovskite three-layer slab offset by 0, $\frac{1}{2}$, 0 relative to the next. The Zr-S distances

TABLE III
SELECTED BOND DISTANCES (Å) AND ANGLES (°)
FOR $Ba_4Zr_3S_{10}$

Zr(1)-S(1)	2.495(5)
Zr(1)-S(3)	2.4899(3)
Zr(2)-S(1)	2.562(5)
Zr(2)-S(2)	2.495(5)
Zr(2)-S(4)	2.4925(4)
Ba(1)-S(1)	3.5157(5)
	3.5276(7)
Ba(1)-S(3)	3.516(1)
Ba(1)-S(4)	3.505(3)
Ba(2)-S(2)	3.540(1)
	3.084(5)
	3.552(1)
Ba(2)-S(4)	3.135(3)
S(1)-Zr(1)-S(1)	180
S(1)-Zr(1)-S(3)	90
S(3)-Zr(1)-S(3)	90
	180
S(1)-Zr(2)-S(2)	180
S(1)-Zr(2)-S(4)	87.5(1)
	92.5(1)
S(4)-Zr(2)-S(4)	89.8(2)
	175.1(2)
S(1)-Ba(1)-S(1)	179.6(2)
S(1)-Ba(1)-S(3)	60.2(1)
	120.2(1)
S(1)-Ba(1)-S(4)	59.7(1)
	119.9(1)
S(3)-Ba(1)-S(3)	90.19(2)
	60.2(3)
S(3)-Ba(1)-S(4)	180
	89.6(1)
	119.8(2)
S(4)-Ba(1)-S(4)	90.5(1)
	60.2(3)
S(2)-Ba(2)-S(2)	166.6(2)
	83.3(1)
	89.2(1)
S(2)-Ba(2)-S(4)	63.2(1)
	127.1(1)
S(4)-Ba(2)-S(4)	94.4(2)
	64.1(3)
Zr(1)-S(1)-Ba(1)	89.8(1)
Zr(2)-S(1)-Ba(1)	90.2(1)
Zr(2)-S(2)-Ba(2)	180
	83.3(1)
Zr(2)-S(4)-Ba(2)	88.4(3)

average 2.493(3) Å with the exception of the long Zr(2)-S(1) contact of 2.562(5) Å. The Ba-S contacts to the 12 coordinate Ba atoms within the perovskite blocks range between 3.505(3) Å and 3.5276(7) Å whereas

the Ba-S contacts to the 9 coordinate Ba atoms in the double rock salt layers range between 3.084(5) and 3.552(1) Å.

Discussion

The $n = 3, 4,$ and 5 members of the $Ba_{n+1}Hf_nS_{3n+1}$ phases have all been prepared from a 3 : 2 : 4 ratio of BaS/Hf/S with varying weight percents of BaCl₂ flux. The present $n = 3$ phases formed with 15 wt% BaCl₂ flux whereas the $n = 4$ and 5 members were isolated from reactions incorporating 25 wt% BaCl₂ (7). Although many factors may influence the course of reaction (e.g., quench conditions, tube size, etc.), the amount of BaCl₂ appears to affect the final product distribution.

The three $Ba_{n+1}M_nS_{3n+1}$ phases with $n \geq 3$ structurally characterized to date (single crystal data) have shown $Fmmm$ crystal symmetry whereas the $n = 2$ and $n = 1$ phases have been refined with $Cccm$ and $I4/mmm$ symmetry, respectively. Our reinvestigation of $Ba_3Zr_2S_7$ from single crystal X-ray diffraction reveals $I4/mmm$ symmetry (12) and delineates the crossover from tetragonal to orthorhombic symmetry in the $Ba_{n+1}Zr_nS_{3n+1}$ series. The structural data for the $Ba_{n+1}M_nS_{3n+1}$ compounds prepared thus far are summarized in Table IV.

The six compounds that have been structurally characterized show a common distortion in the MS_6 octahedra at the perovskite/double BaS interface. The $M-S$ bond distal to the double BaS layer (Fig. 2) is 0.04 to 0.18 Å longer than the other $M-S$ distances, whereas the proximal $M-S$ contacts are equal in length to the other $M-S$ distances in the compounds (Table IV). The $M-S$ contacts in the $a-b$ plane are highly compressed in the $n = 1$ phases but significantly less distorted in the higher n members of the series. The axial Ba-S contacts average 3.1 Å and are in fact shorter than the 6 coordinate Ba-S contacts of 3.193 Å in cubic BaS (13). Short axial $A-X$ contacts ap-

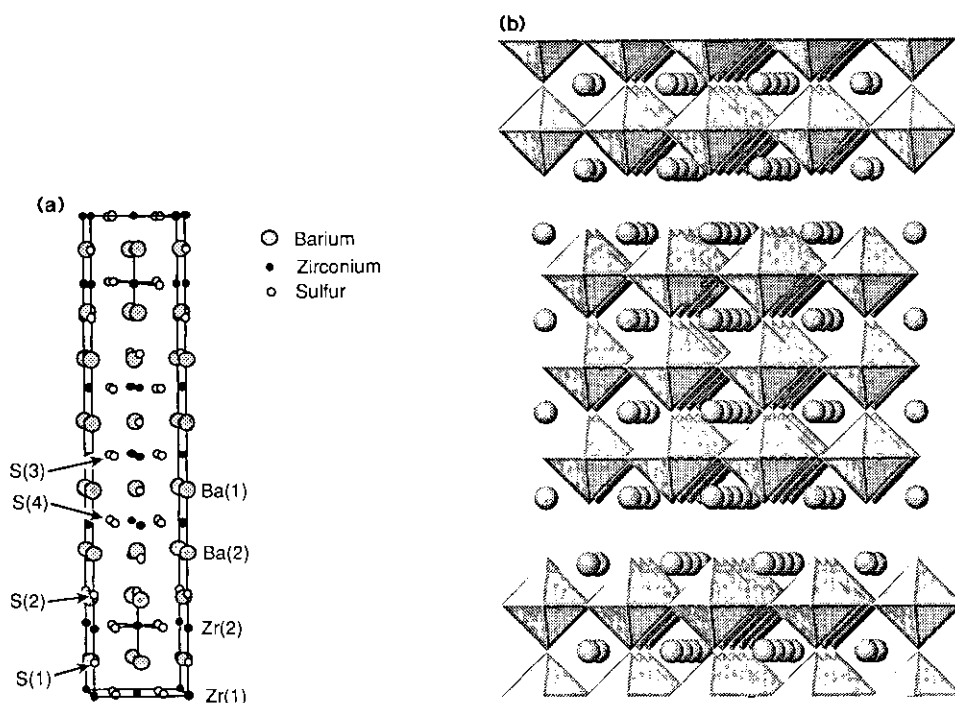


FIG. 1. (a) Ball-and-stick drawing of the $Ba_4Zr_3S_{10}$ unit cell and (b) polyhedral representation showing $ZrS_{6/2}$ octahedra and Ba atoms (shaded balls).

pear to be a common feature in the oxide R-P phases as well (10, 14–16).

The $Cccm$ refinement of $Ba_3Zr_2S_7$ was

suggestive of a structure with buckled ZrS_6 octahedra without Zr–S bond asymmetries; however, a $BaCl_2$ flux synthesis (12) of the

TABLE IV
SUMMARY OF STRUCTURAL DATA^a FOR THE $Ba_{n+1}M_nS_{3n+1}$ PHASES

M	n	$c(\text{Å})$	$a(\text{Å})^b$	$b(\text{Å})$	Space group	Ba–S _c ^c (Å)	Ba–S _{ab} (Å)	M–S _c (Å)	M–S _{ab} (Å)	M–S _{dist} (Å)	Ref.
Hf	1	15.842(3)	6.8369(6)	—	$I4/mmm$	3.13(1)	3.430(4)	—	2.417(1)	2.53(3)	(6)
Zr	1	16.023(2)	6.6686(3)	—	$I4/mmm$	3.18(1)	3.341(2)	—	2.3577(1)	2.52(1)	(6)
Zr	1	15.9641(3)	6.7673(2)	—	$I4/mmm$	3.08(2)	3.399(2)	—	2.393(2)	2.61(2)	(5)
Zr ^d	2	25.4923(7)	7.0697(2)	7.0269(2)	$Bbmb$	3.07(1)	3.55(3)	2.53(1)	2.55(1)	2.538(5)	(5)
Zr	2	25.502(4)	7.0687(9)	—	$I4/mmm$	3.073(8)	3.44(9)	2.501(1)	2.502(7)	2.539(2)	(12)
Hf	3	35.428(8)	6.989(3)	7.022(2)	—	—	—	—	—	—	^e
Zr	3	35.544(7)	7.0314(5)	7.0552(7)	$Fmmm$	3.084(5)	3.546(6)	2.495(5)	2.491(3)	2.562(5)	^e
Hf	4	45.280(5)	6.977(1)	7.006(2)	$Fmmm$	3.082(8)	3.52(1)	2.48(1)	2.471(2)	2.55(1)	(7)
Hf	5	55.205(6)	7.002(1)	6.987(2)	$Fmmm$	3.09(2)	3.520(5)	2.48(2)	2.474(3)	2.53(2)	(7)

^a Subscripts c and ab denote distances along the crystallographic c direction and ab plane, respectively. $M-S_{dist}$ is the distal metal–sulfur distance (see text and Fig. 2). Distances averaged where appropriate.

^b For the tetragonal structures, the a parameters were multiplied by $\sqrt{2}$ for comparison.

^c Excluding the distal $M-S$ distance.

^d b and c parameters were exchanged for comparison and the cell transformed from $Cccm$.

^e This work.

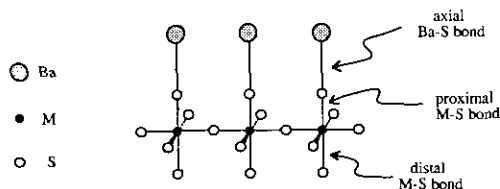


FIG. 2. Schematic representation of the corner shared $ZrS_{6/2}$ octahedra and Ba atoms at the perovskite/double BaS layer interface for the $Ba_{n+1}M_nS_{3n+1}$ phases.

same compound produced a higher symmetry structure with asymmetries identical to those just described.

Acknowledgments

This work was supported by the National Science Foundation (DMR-8913906), the Exxon Education Foundation, and the Center for Superconductivity Research and Department of Chemistry, University of Maryland.

References

1. G. A. WIEGERS AND A. MEERSCHAUT, *J. Alloys Comp.* **178**, 351 (1992), and references therein.
2. K. MATSUURA *et al.*, *J. Solid State Chem.* **94**, 294 (1991).
3. M. ONODA, K. KATO, Y. GOTOH, AND Y. OOSAWA, *Acta Crystallogr. Sect. B* **46**, 487 (1990).
4. P. RABU, A. MEERSCHAUT, J. ROUXEL, AND G. A. WIEGERS, *J. Solid State Chem.* **88**, 451 (1990).
5. M. SAEKI, Y. YAFIMA, AND M. ONODA, *J. Solid State Chem.* **92**, 286 (1991).
6. B.-H. CHEN AND B. W. EICHHORN, *Mater. Res. Bull.* **26**, 1035 (1991).
7. B.-H. CHEN, B. W. EICHHORN, AND P. E. FANWICK, *Inorg. Chem.* **31**, 1788 (1992).
8. S. N. RUDDLESSEN AND P. POPPER, *Acta Crystallogr.* **11**, 54 (1958).
9. R. J. CAVA, B. BATLOGG, R. B. VAN DOVER, J. J. KRAJEWSKI, J. V. WASZCZAK, R. M. FLEMING, W. F. PECK, L. W. RUPP, P. MARSH, A. X. W. P. JAMES, AND L. F. SCHNEEMEYER, *Nature* **345**, 602 (1990).
10. (a) M. ITOH, M. SHIKANO, R. LIANG, H. KAWAJI, AND T. NAKAMURA, *J. Solid State Chem.* **88**, 597 (1990); (b) W. GONG, J. S. XUE, AND J. E. GREEDAN, *J. Solid State Chem.* **91**, 180 (1991).
11. D. T. CROMER, AND J. T. WABER, "International Tables for X-Ray Crystallography," Vol. IV, Table 2.2B, Kynoch, Birmingham (1974).
12. B.-H. CHEN, B. W. EICHHORN, AND W. WONG-NG, to be published.
13. (a) Natl. Bur. Stand. (U.S.), Circ. 539, 7 (1957); (b) JCPDS-ICDD card #8-454.
14. B.-H. CHEN, AND B. W. EICHHORN, *J. Solid State Chem.* **97**, 340 (1992).
15. G. LE FLEM AND P. HAGENMULLER, *J. Solid State Chem.* **38**, 34 (1981).
16. P. GANGULY, AND C. N. R. RAO, *J. Solid State Chem.* **53**, 193 (1984).